

# Approach Guidance to Circular Flight Paths

F. H. KISHI\* AND I. PFEFFER†

TRW Inc., Redondo Beach, Calif.

A novel technique for guiding an aircraft from a distant point to a given circular orbit over a fixed ground area is presented. The avionics system required to perform this guidance would consist of a sensor which tracks a ground reference point to give pointing data in aircraft coordinates, and vertical and directional gyros to give bank and heading information. The system requires a computer (which solves the guidance problem in real time) and a display (which presents bank angle commands to the pilot). This paper is primarily devoted to the guidance required for a smooth, rapid approach to the desired orbit in spite of system constraints such as sensor gimbal limits and bank and bank rate limits. A computer simulation is made of the system and typical trajectories derived from the chosen guidance philosophy are shown. Comparisons are also given between the chosen guidance scheme and theoretical optimums.

## Nomenclature

$g$	= gravity
$h, k$	= displacement of aircraft turn center with respect to target center
$H$	= altitude
$R_c$	= slant range to target
$r_d$	= radius of desired cruise orbit, horizontal plane
$t$	= time
$V$	= true airspeed
$x_b, y_b, z_b$	= target position in body coordinates
$x_c, y_c, z_c$	= target position in Earth coordinates
$\dot{x}_c, \dot{y}_c$	= aircraft velocity components in Earth coordinates
$x_0, y_0$	= phase plane coordinates
$x_{0n}, y_{0n}$	= normalized phase plane coordinates
$\phi$	= bank angle
$\dot{\phi}$	= bank rate
$\phi_e$	= roll error
$\phi_g$	= sensor gimbal angle, elevation
$\psi_g$	= sensor gimbal angle, azimuth
$\rho$	= turn radius
$\tau_{ar}$	= aircraft response delay (including pilot delay)
$\theta_h$	= aircraft heading
$\dot{\theta}_h$	= aircraft turning rate

## Introduction

ONE can imagine many applications where it is desired to maneuver an aircraft into a circular cruise orbit about some point on the ground. Examples are reconnaissance of a ground point by side-looking cameras or sensors, parking orbits for aircraft waiting to land, and aircraft receiving information transmitted from the ground to retransmit to other ground points. This paper provides an analytical tool to design the guidance system which will perform the approach maneuver.

The first section states the problem, followed by a section presenting the "phase" plane which is introduced to help solve the problem. A solution to the approach problem is then given, followed by equations to maintain the gimbal angles of a sensor tracking a ground point within its limits. Finally, the last section describes a timeshare computer simulation with typical runs.

Received September 8, 1969; presented as Paper 69-986 at the AIAA Aerospace Computer Systems Conference, Los Angeles, Calif., September 8-10, 1969; revision received February 25, 1970.

\* Senior Staff Engineer, Advanced Electronic Systems Operation.

† Manager of Technical Staff, Advanced Electronic Systems Operation. Member AIAA.

## Problem Statement

The problem, shown pictorially in Fig. 1, is that of determining steering signals that maneuver the airplane from an arbitrary starting point to a cruise orbit around a target center in minimum time. The following assumptions are made: 1) The aircraft heading and bank angle are known continuously in time. 2) The aircraft flies always in a coordinated turn. 3) The aircraft flies a given constant altitude and a given constant true airspeed. 4) Sensor gimbal angles are known continuously in time in order to determine aircraft position with respect to the target. An inertial reference unit can be used in place of the gimbal angles, as the important parameters are the relative position of the aircraft and target. 5) The specific heading angle at the time of entry into the cruise orbit is unimportant. 6) The sensor is limited to viewing an area to the left of the airplane with the forward azimuth gimbal angle limited to a specified value. This assumption restricts final cruise orbits to be in left bank. 7) The radius of the desired cruise orbit in the horizontal plane is given and equal to  $r_d$ .

Referring to Fig. 2 for convention, the target position in body coordinates ( $b$  subscripts) is found by

$$x_b = R_c \cos \phi_g \cos \psi_g, y_b = -R_c \cos \phi_g \sin \psi_g, z_b = R_c \sin \phi_g$$

The target position in coordinates referenced to Earth ( $c$  subscripts) is then given by the transformation

$$\begin{bmatrix} x_c \\ y_c \\ z_c \end{bmatrix} = \begin{bmatrix} \cos \theta_h & \sin \theta_h & 0 \\ -\sin \theta_h & \cos \theta_h & 0 \\ 0 & 0 & 1 \end{bmatrix} \begin{bmatrix} \cos \phi & 0 & \sin \phi \\ 0 & 1 & 0 \\ -\sin \phi & 0 & \cos \phi \end{bmatrix} \begin{bmatrix} x_b \\ y_b \\ z_b \end{bmatrix}$$

The fact that  $z_c$  is equal to  $(-H)$  allows solution for  $R_c$

$$R_c = -H / (-\sin \phi \cos \psi_g \cos \phi_g + \cos \phi \sin \phi_g)$$

The problem then resolves to one of knowing  $\theta_h$ ,  $\phi$ ,  $x_c$ ,  $y_c$  continuously in time and finding the steering signal (roll error) that will accomplish the approach maneuver. The approach system is shown schematically in Fig. 3.

In the approach calculations, all lateral maneuvers are assumed to be performed in a coordinated turn, i.e., no yaw maneuvers. This implies that the velocity vector is in the direction of the longitudinal axis, and the lateral acceleration is given by  $g \tan \phi = V^2/\rho$ .

## Phase Plane

A new coordinate system ( $x_0, y_0$ ) is defined in the horizontal plane, which has its origin at the cruise orbit center. The  $y_0$

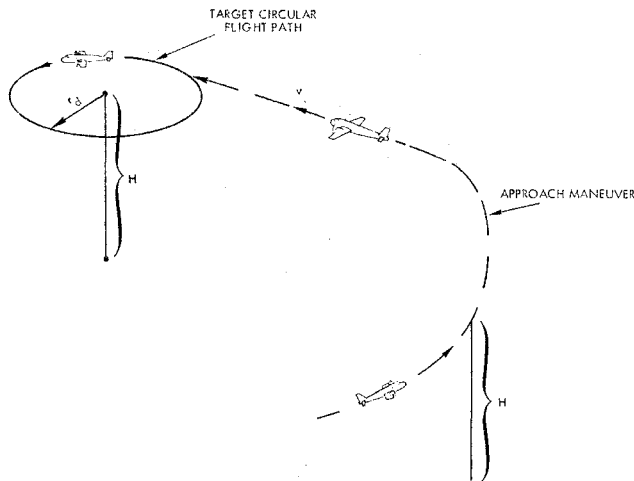


Fig. 1 Basic maneuver geometry.

axis points in the same direction as the aircraft heading, and the  $x_0$  axis is orthogonal to  $y_0$  and is positive to the right when looking in the direction of  $y_0$ . In this plane, designated the phase plane, the destination becomes  $x_0 = r_d$  and  $y_0 = 0$ . The aircraft is located in this plane by the transformation

$$x_0 = x_c \cos \theta_h - y_c \sin \theta_h, y_0 = x_c \sin \theta_h + y_c \cos \theta_h$$

The displacement of the aircraft from  $(r_d, 0)$  can be viewed as an error which we desire to reduce to zero rapidly.

When  $x_0$  and  $y_0$  are transformed into polar coordinates  $(r, \theta)$ , lines of constant  $r$  (concentric circles) are lines of equal position error, whereas lines of constant  $\theta$  (radial lines) are lines of equal velocity error. Since this plane can be obtained by conformal transformation from the phase plane<sup>1</sup> utilized in control systems theory, we have adopted the designation phase plane, with the  $z$  (in phase) used because of the  $z$  plane analogy<sup>1</sup> also used in control systems theory (constant  $\sigma$  lines and constant  $\omega$  lines become, respectively in the  $z$  plane, concentric circles and radial lines).

The following two theorems allow mapping real-world trajectories when they are composed of constant bank turns and determine time spent along various paths. The proofs are given in Appendix A.

**Theorem 1:** Given a constant bank turn which describes in an Earth-fixed coordinate a circle of radius  $\rho$  and center  $(h, k)$  with respect to the cruise orbit center. The trajectory described in the phase plane is a circle with center at  $x_0 = \rho$ ,  $y_0 = 0$ , and radius of  $(h^2 + k^2)^{1/2}$ . (Zero bank can be in-

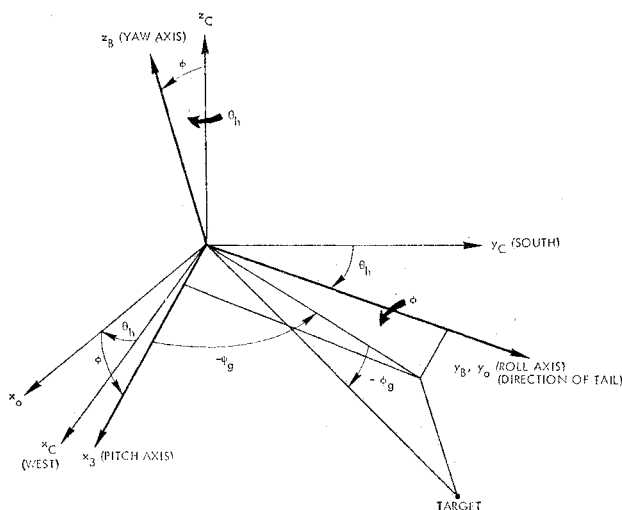


Fig. 2 Earth and body coordinate systems and bank heading and gimbal angle definition.

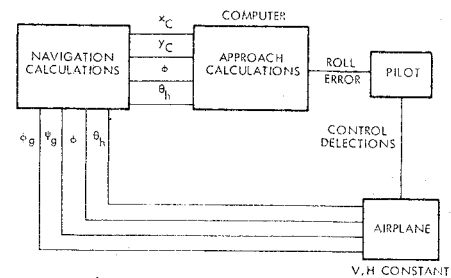


Fig. 3 Approach problem block diagram.

terpreted as having  $\rho = \infty$ , in which case the trajectories are lines parallel to the  $y_0$  axis.)

**Theorem 2:** For the constant bank turn, the distance  $d$  traveled in the normal plane in  $\Delta T$  seconds is multiplied by the ratio  $(h^2 + k^2)^{1/2}/\rho$  to obtain the corresponding displacement in the phase plane.

Utilizing these theorems, design of an approach computer algorithm can be performed, as will be shown in the next section.

### A Solution

With a knowledge of how phase plane trajectories can be drawn for constant bank turns, this plane is divided into several regions within which different bank commands are implemented. The problem becomes one of selecting the bank angle levels and the location of borders. The choices are somewhat arbitrary, however, at regions far from the destination, the bank levels are chosen at the limits within which we desire to operate. As a guide to the selection of the borders, optimal solutions to simplified forms of the real problem (as given in Appendix B) can be used. In actual practice, the final selections are made based on such factors as undesirability of large bank angle changes and gimbal angle limitations.

To illustrate how a selection would be made, let us assume some numbers. Let  $V = 274$  ft/sec,  $g = 32.2$  ft/sec<sup>2</sup>, and  $r_d = 4000$  ft; then the bank angle at the destination is  $30.237^\circ$ . The phase plane can be normalized by  $r_d = 4000$ , which causes the destination to become  $x_{0n} = 1$ ,  $y_{0n} = 0$  (subscript  $n$  referring to normalized coordinates).

The optimum solution, assuming no roll dynamics and no gimbal limits, depends upon the selected bank angle limits. Several solutions are obtained in Appendix B with the result of particular interest to the present discussion shown in Fig. 13 for bank limits of  $0 \leq \phi \leq 30.237$ . Of course, widening the limits of the bank angle dynamic range will result in faster approaches.

Using Fig. 13 as a crude guide, one simple solution is shown in Fig. 4, with the same figure containing some arcs of trajectories shown in Fig. 5. For  $y_0 < 0$  and large  $x_0$ , a similar re-

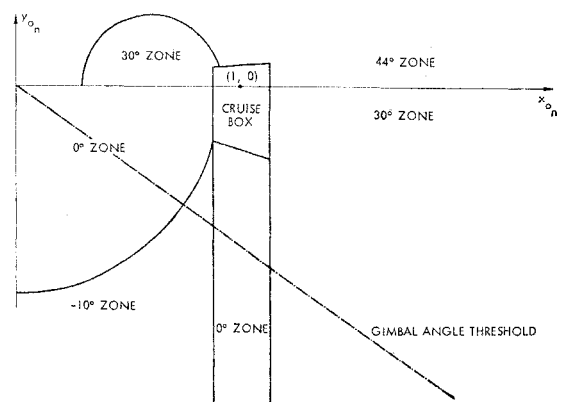


Fig. 4 A solution in phase plane.

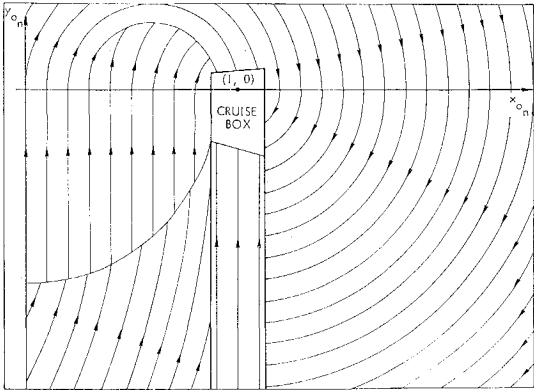


Fig. 5 Trajectories in phase plane.

sponse to the optimum is obtained. The 44° zone is added to speed the response, but this level is not continued to avoid the large transition from 44 to 0°. A -10° zone is added to speed the response; however, a 0° zone is added to avoid large elevation gimbal deflections. Finally, the 30° zone for  $y_0 > 0$  is added to ease the transition from 0 to 44°. Approach guidance is assumed completed when the aircraft is taken into the cruise box, at which time another control law can take over to perform the final maneuver and to maintain the aircraft close to the cruise orbit. (This control can be simply obtained by measuring the radial distance from the orbit center and building a closed-loop system based on the error from  $r_d$ .)

In Fig. 5, and as determined by Theorem 1, 30° arcs have their center at (1,0); 44° arcs have a center at (0.6,0); and -10° arcs have a center at (-3.3,0). It is noted that trajectories starting from any point in the phase plane eventually terminate in the cruise box. Also along the borders, the direction of the paths on one side of a border is not opposed by the paths on the other side. If this situation occurred, a stalemate would result, with no advancement to the destination. It is noted that the 30° bank for  $y_0 < 0$  cannot be replaced by anything less without creating a stalemate along the  $y_0 = 0$  line.

Gimbal Limit Following Equations

Straight line trajectories in the phase plane other than those parallel to  $y_0$  can be obtained by continuously calculating the bank angle required to maintain the trajectory along a specified straight line. This observation can be utilized whenever sensor gimbal angle limits are present. A line is drawn from the cruise center (assuming that the sensor is tracking the cruise center) at an angle slightly less than the gimbal limit down from the  $x_0$  axis. Whenever the no-limit command obtained in the last section requires the trajectory to go below this threshold line, an alternate command calculation is performed to cause the trajectory to follow this line until the no-limit command is less than the gimbal limit command, at which time the no-limit command is again used.

To derive the gimbal limit following equations, we refer to Fig. 6. Noting similar triangles, the turn radius is given by

$$\rho = x_0 + (y_0)^2/x_0$$

or the commanded bank angle is given by

$$\tan \phi = (V^2/g)[x_0/(x_0^2 + y_0^2)]$$

Computer Simulation

The closed-loop approach guidance shown in Fig. 3 can readily be simulated on a timeshare computer. A summary of the equations used and typical results are presented in this section.

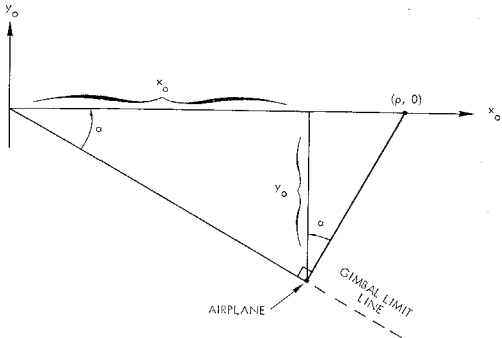


Fig. 6 Determination of turn radius to fly along gimbal limit line.

Navigation Calculations: (The equations were derived in the problem statement section.)

$$R_c = -H/(-\sin \phi \cos \psi_\theta \cos \phi_\theta + \cos \phi \sin \phi_\theta)$$
$$x_c = R_c[\cos \phi \cos \theta_h \cos \phi_\theta \cos \psi_\theta - \sin \theta_h \cos \phi_\theta \sin \psi_\theta + \sin \phi \cos \theta_h \sin \phi_\theta]$$
$$y_c = R_c[-\cos \phi \sin \theta_h \cos \phi_\theta \cos \psi_\theta - \cos \theta_h \cos \phi_\theta \sin \psi_\theta + \sin \phi \sin \theta_h \sin \phi_\theta]$$

Approach Calculations: The algorithm is shown in Fig. 7.

Pilot: The pilot is simulated as a simple lag which is incorporated with the aircraft response.

Airplane Dynamics: The bank rate is given by  $\dot{\phi} = \phi_c/\tau_{ar}$ . The turning rate of the aircraft is  $\dot{\theta}_h = -(g/V) \tan \phi$ . The velocity components in the earth-fixed coordinate system are

$$\dot{x}_c = V \sin \theta_h$$
$$\dot{y}_c = V \cos \theta_h$$

Integration yields position components. The inverse of the navigation calculations then yields the gimbal angles, which are fed into the navigation calculations. Without any sensor noise considerations, the position components can be fed directly into the approach calculations. Of course, the airplane and pilot simulation can be made much more compli-

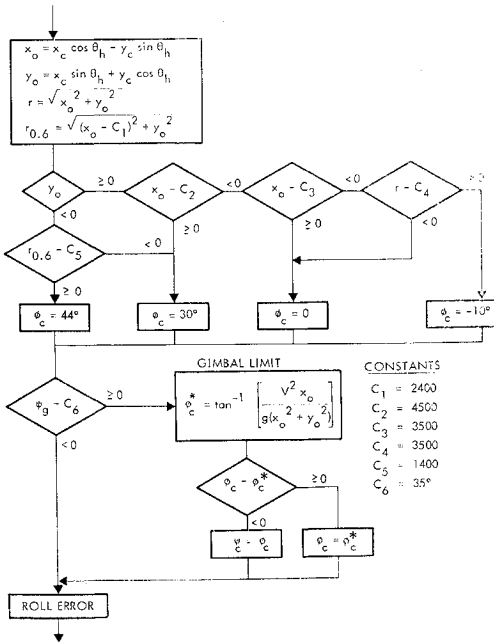


Fig. 7 Approach algorithm.

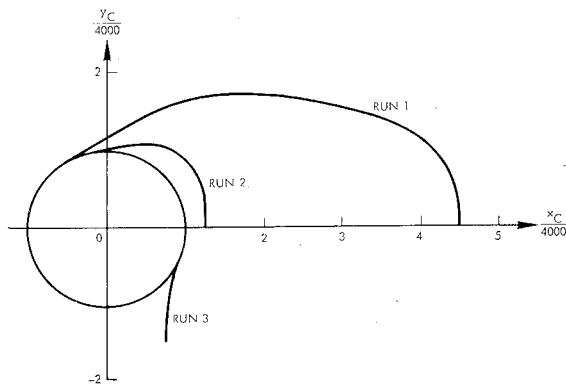


Fig. 8 Approach trajectories in Earth coordinates.

cated inserting quantities such as angles of attack and wind uncertainties.

Typical results are shown in Tables 1, 2, and 3, and in Fig. 8. The tables show the approaches both in the Earth-fixed and the phaze plane, whereas the trajectory in the Earth-fixed coordinates is plotted in the figure. These runs were made assuming an aircraft response delay of one second and a roll rate limit of  $5^\circ/\text{sec}$ . The gimbal limit threshold is set at  $35^\circ$ , which causes gimbal angles to stay below  $45^\circ$ . Run 1 shows probably the most common approach that will be encountered. The run starts in the  $30^\circ$  region, encounters the gimbal limit threshold, rides along this line for the major portion of the run, and enters the  $0^\circ$  zone just prior to capturing in the cruise box. Run 2 shows a case starting closer to the encountering point. Run 3 shows a case starting in the  $-10^\circ$  zone assuming for this case that no gimbal limit is present. In all of the runs, it is shown that the trajectories approach the destination of  $(x_0, y_0)$  equal to  $(4000, 0)$ .

A comparison between Run 1 of the chosen guidance scheme and some theoretical results (found in Appendix B) is shown in Fig. 9, with the approach times tabulated on the figure. Of course, the theoretical optimums are dependent upon the dynamic range of the bank angle. The judgment of the chosen scheme in the above comparison should be tempered by the fact that the optimum results do not consider gimbal limits or roll dynamics. The arched trajectory for the chosen scheme is necessary to satisfy the azimuth gimbal limit.

### Conclusion

The phaze plane introduced in this paper is shown to be a convenient analytical tool for designing approach guidance equations for aircraft that are required to go into a circular cruise orbit about a fixed ground area. The design can be aided by theoretical minimum time solutions.

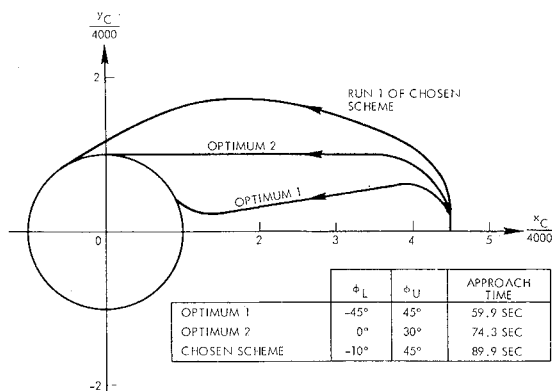


Fig. 9 Comparison of the chosen scheme with theoretical optimums.

Table 1 Run 1

$t$ (sec)	$\theta_h$ (deg)	$\phi$ (deg)	$x_c$ (ft)	$y_c$ (ft)	$x_0$ (ft)	$y_0$ (ft)	$\psi_\theta$ (deg)
0	0	0	18,000	0	18,000	0	0
7.2	-13.4	29.0	17,856	1953	17,869	-1,934	6.0
14.4	-41.4	30.0	16,962	3680	15,362	-8,181	27.0
21.6	-63.4	9.8	15,381	4821	11,291	-11,602	43.6
28.8	-68.9	6.1	13,584	5611	10,182	-10,698	45.0
36.0	-74.3	6.7	11,723	6232	9,215	-9,657	44.6
43.2	-80.4	7.5	9,808	6663	8,249	-8,615	44.1
50.4	-87.3	8.6	7,857	6875	7,285	-7,577	43.4
57.6	-95.2	9.9	5,896	6836	6,324	-6,541	42.4
64.8	-104.4	11.7	3,962	6507	5,365	-5,508	40.9
72.0	-115.4	11.9	2,117	5844	4,412	-4,477	40.0
79.2	-119.6	2.0	386	4919	4,089	-2,858	33.7
86.0 <sup>a</sup>	-120.7	1.0			4,047	-1,075	

A suggestion for further study in this area would be an exploration of minimum fuel trajectories. Such a consideration would be important if the fuel flow rate is strongly dependent on the bank angle. With no dependence minimum time yields minimum fuel.

### Appendix A

Proofs are given for the two theorems stated in the text.

#### Proof of Theorem 1

The relevant coordinate systems are shown in Fig. 10. In the  $x'_0, y'_0$  axes, which are in the same directions as  $x_0, y_0$ , the coordinates of the aircraft are  $(\rho, 0)$ . In  $x', y'$  coordinates, the aircraft is

$$\begin{bmatrix} x' \\ y' \end{bmatrix} = \begin{bmatrix} \cos\theta_h & \sin\theta_h \\ -\sin\theta_h & \cos\theta_h \end{bmatrix} \begin{bmatrix} \rho \\ 0 \end{bmatrix}$$

In the  $(x, y)$  coordinate system,

$$\begin{bmatrix} x \\ y \end{bmatrix} = \begin{bmatrix} x' + h \\ y' + k \end{bmatrix}$$

Finally, in the  $(x_0, y_0)$  coordinate system,

$$\begin{bmatrix} x_0 \\ y_0 \end{bmatrix} = \begin{bmatrix} \rho \\ 0 \end{bmatrix} + \begin{bmatrix} \cos\theta_h & -\sin\theta_h \\ \sin\theta_h & \cos\theta_h \end{bmatrix} \begin{bmatrix} h \\ k \end{bmatrix}$$

or,

$$x_0 - \rho = h \cos\theta_h - k \sin\theta_h, \quad y_0 = h \sin\theta_h + k \cos\theta_h$$

Squaring and adding the two equations yields

$$(x_0 - \rho)^2 + y_0^2 = h^2 + k^2$$

This is an equation of a circle with center at  $(\rho, 0)$  and radius equal to  $(h^2 + k^2)^{1/2}$ .

#### Proof of Theorem 2

We consider a distance  $d$  traveled in a given time  $(t_2 - t_1)$  in the Earth-fixed coordinate  $(x, y)$  and determine the corresponding displacement in the  $(x_0, y_0)$  plane. Figure 11 is shown to assist the discussion. Time instant  $t_1$  is indicated by the subscript 1 and time instant  $t_2$  is indicated by the subscript 2.

The  $(x', y')$  coordinates of the aircraft at  $t_1$  are given by

$$x'_1 = \rho \cos(-\theta_h), \quad y'_1 = \rho \sin(-\theta_h)$$

Table 2 Run 2

$t$ (sec)	$\theta_h$ (deg)	$\phi$ (deg)	$x_c$ (ft)	$y_c$ (ft)	$x_0$ (ft)	$y_0$ (ft)	$\psi_\theta$ (deg)
0	0	0	5000	0	5000	0	0
7.2	-13.8	32.8	4855	1953	5161	780	-6.1
14.4	-52.1	31.0	3790	3554	5153	-773	6.1
21.6	-80.4	30.0	2011	4335	4641	-1243	10.4
27.0 <sup>a</sup>	-96.6	15.1					

Table 3 Run 3<sup>b</sup>

$t$ (sec)	$\theta_h$ (deg)	$\phi$ (deg)	$x_c$ (ft)	$y_c$ (ft)	$x_0$ (ft)	$y_0$ (ft)	$\psi_g$ (deg)
0	0	0	3000	-6000	3,000	-6000	
7.2	6.6	-9.9	3092	-4040	3,510	-3780	56.5
14.4	12.3	-4.4	3429	-2107	3,795	-1437	23.2
15.84 <sup>a</sup>	12.9	-4.1			3,810	-996	

<sup>a</sup> Capture in cruise box.<sup>b</sup> Run assuming no gimbal limits.

In the  $(x_0, y_0)$  coordinates, the same point is given by

$$\begin{aligned} x_{01} &= \rho + h \cos(-\theta_h) + k \sin(-\theta_h), \\ y_{01} &= -h \sin(-\theta_h) + k \sin(-\theta_h) \end{aligned}$$

The  $(x', y')$  coordinates of the aircraft at  $t_2$  are given by

$$x_2' = \cos[-\theta_h + (d/\rho)], \quad y_2' = \sin[-\theta_h + (d/\rho)]$$

In the  $(x_0, y_0)$  coordinates the same point is given by

$$\begin{aligned} x_{02} &= \rho + h \cos[-\theta_h + (d/\rho)] + k \sin[-\theta_h + (d/\rho)] \\ y_{02} &= -h \sin[-\theta_h + (d/\rho)] + k \cos[-\theta_h + (d/\rho)] \end{aligned}$$

Subtracting the coordinates of the two points, squaring, and adding yields

$$\begin{aligned} [x_{02} - x_{01}]^2 + [y_{02} - y_{01}]^2 &= \\ [h^2 + k^2] \{ \cos[-\theta_h + (d/\rho)] - \cos[-\theta_h] \}^2 + \\ &\quad \{ \sin[-\theta_h + (d/\rho)] - \sin[-\theta_h] \}^2 \end{aligned}$$

or,

$$[(x_{02} - x_{01})^2 + (y_{02} - y_{01})^2]^{1/2} = [(h^2 + k^2)^{1/2}/\rho]d$$

The displacement  $d$  in the Earth-fixed plane is multiplied by  $(h^2 + k^2)^{1/2}/\rho$  to obtain the corresponding displacement in the phase plane.

## Appendix B

The minimum time guidance problem is stated; and, to justify somewhat the control logic in the text, a discussion is given of typical minimum time solutions. Also, the use of the coordinate transformation which converts the problem to the phase coordinates is shown to simplify the problem formulation and solution.

### Minimum Time Guidance Problem

Find the piecewise continuous function  $\phi(t)$  over the interval  $[0, t_f]$  which will take the state from  $[x_c(0), y_c(0)]$  to a final condition given by

$$[x_c^2(t_f) + y_c^2(t_f)]^{1/2} = r_d, \quad x_c(t_f)\dot{x}_c(t_f) + y_c(t_f)\dot{y}_c(t_f) = 0$$

in minimum time, while satisfying

$$\begin{aligned} \dot{x}_c &= V \sin \theta_h \quad [V \text{ is a known constant}] \\ \dot{y}_c &= V \cos \theta_h \\ \dot{\theta}_h &= -(g/V) \tan \phi \quad [g \text{ is a known constant}] \\ \phi_L &\leq \phi \leq \phi_u \quad [\phi_L, \phi_u \text{ are known constants}] \end{aligned}$$

Let  $u(t) = (g/V) \tan \phi(t)$ , then, if we find  $u(t)$ ,  $\phi(t)$  is known. An equivalent constraint appears on  $u(t)$ .

$$u(t) \leq u_u = (g/V) \tan \phi_u, \quad u(t) \leq u_L = (g/V) \tan \phi_L \quad (1)$$

The coordinate transformation between  $(x_c, y_c)$  and the phase coordinates  $(x_0, y_0)$  is

$$x_0 = x_c \cos \theta_h - y_c \sin \theta_h, \quad y_0 = x_c \sin \theta_h + y_c \cos \theta_h \quad (2)$$

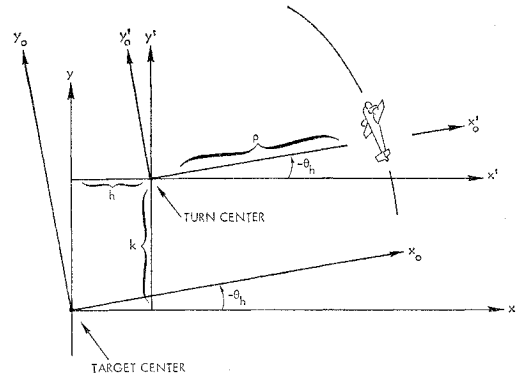


Fig. 10 Coordinates used in the proof of theorem 1.

Differentiating these equations yields

$$\dot{x}_0 = y_0 u, \quad \dot{y}_0 = -x_0 u + V \quad (3)$$

in terms of which we can restate the problem.

### Equivalent Minimum Time Guidance Problem

Find the piecewise continuous function  $u(t)$  defined over the interval  $[0, t_f]$  which will take the state from  $[x_0(0), y_0(0)]$  to a final state  $(r_d, 0)$  in minimum time while satisfying

$$\dot{x}_0 = y_0 u, \quad \dot{y}_0 = -x_0 u + V, \quad u_L \leq u(t) \leq u_u$$

The initial state  $[x_0(0), y_0(0)]$  is found by inserting  $[x_c(0), y_c(0)]$  into Eq. (2).

We apply Pontryagin's Maximum Principle<sup>2</sup> to obtain optimal solutions. The Hamiltonian is

$$H = (p_1 y_0 - p_2 x_0)u + p_2 V + p_0 \quad (4)$$

where the adjoint variables  $(p_1, p_2)$  satisfy

$$\dot{p}_1 = p_2 u, \quad \dot{p}_2 = -p_1 u, \quad p_0 = -1 \quad (5)$$

and we know that  $H$  is a constant along an optimal solution. This constant is shown to be zero by applying the transversality condition.

From Eqs. (4), the optimal solution  $u^*$  is

$$u^* = \begin{cases} u_u & \text{when } (p_1 y_0 - p_2 x_0) > 0 \\ u_L & \text{when } (p_1 y_0 - p_2 x_0) < 0 \end{cases} \quad (6)$$

The optimal solution for our problem is bang-bang except there is a possibility of singular subarcs<sup>3</sup> when

$$p_1 y_0 - p_2 x_0 = 0 \quad (7)$$

for any nontrivial interval of time.

We first determine solutions along singular subarcs. If Eq. (7) is to be zero for some nontrivial interval of time, then its derivative must also be zero for that interval. Taking the derivative of Eq. (7) yields  $p_1 V = 0$  or  $p_1 = 0$  along singular subarcs.

Inserting this result in Eq. (5), either  $p_2$  is equal to zero or  $p_2$  is equal to a nonzero constant. If  $p_2$  is equal to zero, then the Hamiltonian is equal to  $-1$ , which is a contradiction.

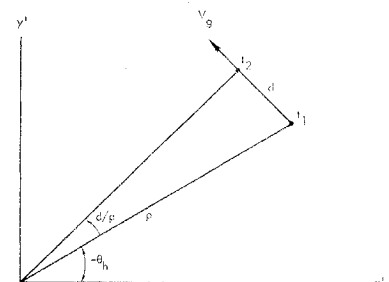


Fig. 11 Coordinates used in the proof of theorem 2.

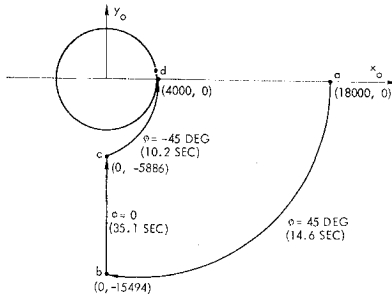


Fig. 12 Example 1: optimal trajectories for  $-45^\circ \leq \Phi \leq +45^\circ$ .

Therefore,  $p_2$  is a nonzero constant, and from Eq. (5) we conclude that the optimal  $u$  is equal to

$$u^*(t) = 0 \text{ along singular subarcs} \quad (8)$$

and  $p_2 = 1/V$  from Eq. (4).

From Eq. (7), we also conclude that

$$x_0^* = 0 \text{ along singular subarcs} \quad (9)$$

This simple result provides probably the greatest single justification for the use of the phase coordinates  $(x_0, y_0)$ .

Segments of optimal trajectories can be determined. During intervals when no switching takes place, the differential equations are given by

$$\dot{x}_0 = \bar{u}y_0, \quad \dot{y}_0 = -\bar{u}x_0 + V \quad (10)$$

$$\dot{p}_1 = \bar{u}p_2, \quad \dot{p}_2 = -\bar{u}p_1 \quad (11)$$

where  $\bar{u}$  is equal to either  $u_u$ ,  $u_L$ , or zero.

Since these equations are linear they can be easily solved. In the forward direction, when  $\bar{u}$  is nonzero,

$$x_0(t) = [x(0) - V/\bar{u}] \cos \bar{u}t + y(0) \sin \bar{u}t + V/\bar{u} \quad (12)$$

$$y_0(t) = y(0) \cos \bar{u}t + [V/\bar{u} - x(0)] \sin \bar{u}t$$

$$p_1(t) = p_1(0) \cos \bar{u}t + p_2(0) \sin \bar{u}t \quad (13)$$

$$p_2(t) = p_2(0) \cos \bar{u}t - p_1(0) \sin \bar{u}t$$

For time running backwards,  $\tau = t_1 - t$ , where  $t_1$  is fixed and  $t$  moves backwards (smaller)

$$x_0(\tau) = [x(0) - V/\bar{u}] \cos \bar{u}\tau - y(0) \sin \bar{u}\tau + V/\bar{u} \quad (14)$$

$$y_0(\tau) = y(0) \cos \bar{u}\tau + [x(0) - V/\bar{u}] \sin \bar{u}\tau$$

$$p_1(\tau) = p_1(0) \cos \bar{u}\tau - p_2(0) \sin \bar{u}\tau \quad (15)$$

$$p_2(\tau) = p_1(0) \sin \bar{u}\tau + p_2(0) \cos \bar{u}\tau$$

where the arguments in  $[x(0), y(0)]$  represent  $\tau = 0$  or  $t = t_1$ .

From Eqs. (12) and (13), it is easily shown that

$$[x_0 - V/\bar{u}]^2 + y_0^2 = [x(0) - V/\bar{u}]^2 + y(0)^2 \quad (16)$$

$$p_1^2 + p_2^2 = p_1^2(0) + p_2^2(0) \quad (17)$$

This provides an alternate proof to Theorem 1 in the text. We note that segments of optimal trajectories in the adjoint space are also arcs of circles.

The solution along intervals when  $u^*$  is equal to zero is given by

$$x_0(t) = \text{const}, \quad p_1(t) = \text{const} \quad (18)$$

$$y_0(t) = \text{const} + Vt, \quad p_2(t) = 1/V$$

We apply our results to two examples.

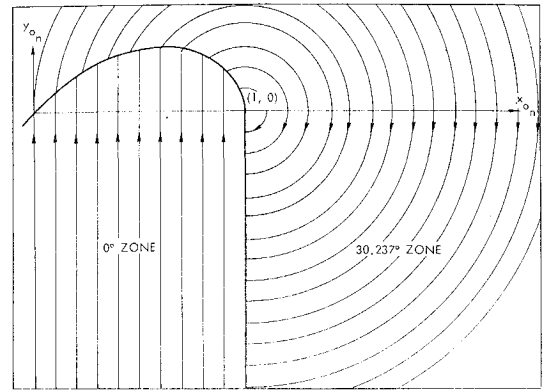


Fig. 13 Optimal State Portrait for  $0 \leq \Phi \leq 30.237^\circ$ .

Example 1: Let us assume that

$$\phi_u = 45^\circ, \quad \phi_L = -45^\circ$$

and we take as a starting point  $x_0 = 18,000$ ,  $y_0 = 0$  with the other constants chosen the same as those used in the case runs in the text:

$$V = 274, \quad g = 32.2, \quad r_d = 4000$$

From Eq. (1)  $u_u = 0.1175$  and  $u_L = -0.1175$ .

The optimal trajectory is shown in Fig. 12. The first arc terminates at the singular subarc at point b. From Eq. (16)

$$y_0^2 = (18000 - 274/0.1175)^2 - (274/0.1175)^2$$

or

$$y_0 = -15494$$

The time taken along this arc is found from Eq. (12),

$$(15494) = (274/0.1175 - 18000) \sin(0.1175t)$$

or

$$t = 14.6 \text{ sec}$$

The final arc, (c - d), is found by working backwards from the final destination using  $u_L$ . This arc terminates at a singular subarc at  $y_0 = -5886$  from Eq. (16). The time taken in this segment is found from Eq. (12),  $t = 10.2$  sec.

Finally, along the singular subarc  $t = (15494 - 5886)/274 = 35.1$  sec. The total time is 59.9 sec. It can be verified that this trajectory satisfies the necessary conditions.

Example 2: This example is the same as Example 1, except

$$\phi_u = 30.237^\circ, \quad \phi_L = 0^\circ$$

and

$$u_u = 0.0685, \quad u_L = 0$$

The solution for this case appears to consist of two arcs, a  $30^\circ$  arc followed by a  $0^\circ$  arc. From Eq. (16), the end of the first arc at  $x_0 = 4000$  is at  $y_0 = -14000$  and the time along the first arc is equal to 23.2 sec. Time along the straight line path is 51.1 sec, giving a total time of 74.3 sec.

The constraint at zero apparently is a situation where Pontryagin's theory does not provide necessary conditions (a condition where  $p_0 = 0$ ). When the  $30^\circ$  arc hits the  $0^\circ$  arc, from Eq. (4)  $p_2 = 1/V$ .

Assuming that  $x_0$ ,  $y_0$ ,  $p_1$ , and  $p_2$  are continuous and taking a time instant just prior to hitting the zero degree arc, we also conclude from Eq. (4) that  $p_1 = x_0/Vy_0$ . Since the final arc  $x_0$  is a constant but  $y_0$  changes, we have to conclude that  $p_1$  is not a constant, which is a contradiction from Eq. (18). This conflict can be avoided by taking the lower control constraint close but not equal to zero, say  $\phi_L = -1^\circ$ . For this case the switching takes place at

$$x_0 = 3287.7, \quad y_0 = -13981.9$$

$$p_1 = 0.868165 \times 10^{-3}, \quad p_2 = 0.36496 \times 10^{-2}$$

and the first arc time equal to 23.7 sec, the final arc equal to 49.8 sec, and a total time of 73.5 sec. The Hamiltonian can be shown to be equal to zero along the trajectory by using the forward and backward solutions of the adjoint variable.

Taking the limit as the lower control constraint is taken to zero, the phase portrait is derived and shown in Fig. 13 for the case with lower control constraint of  $0^\circ$ .

## References

- <sup>1</sup> Truxal, J. G., *Control System Synthesis*, McGraw-Hill, New York, 1955.
- <sup>2</sup> Pontryagin, L. S. et al., *The Mathematical Theory of Optimal Processes*, Wiley, New York, 1962.
- <sup>3</sup> Johnson, C. D., "Singular Solutions in Problems of Optimal Control," *Advances in Control Systems*, edited by C. T. Leondes, Academic Press, New York, 1965.

# Optimum Horizontal Guidance Techniques for Aircraft

HEINZ ERZBERGER\* AND HOMER Q. LEE\*  
NASA Ames Research Center, Moffett Field, Calif.

In the design of advanced flight control systems, consideration is currently being given to the problem of performing various terminal area maneuvers automatically. This paper discusses some problems of automatic guidance of an aircraft in the horizontal plane. The horizontal guidance tasks, which such a flight control system should be capable of performing, have been identified as being of three types: guiding the aircraft from any initial location and initial heading to a) any final location and heading; b) intercept and fly along a line of specified direction; and c) a final location with arbitrary final heading. Guidance problems, such as capturing an ILS beam at a specified point on the beam, intercepting a VOR radial, and point to point navigation, can be formulated in terms of these problems. The guidance laws given in this paper minimize the arc length of the trajectories to fly between initial and final conditions subject to a constraint on the turning radius of the aircraft. Application of the Minimum Principle to these problems has shown that the trajectories consist of a sequence of minimum radius turns and straight-line segments. At most, four partial turns may be required in problem a and two turns in problem b and c. A simple geometric technique is outlined for constructing the optimum trajectories graphically. The optimum control laws are derived for problems b and c.

## Introduction

**F**LIGHT control systems for aircraft are rapidly evolving toward the automation of many traditional piloting functions. Increased automation in flight control systems has been made possible by the advent of flight worthy computers, and is found to be necessary for the safe and economical operation of such advanced aircraft as the SST and some V/STOL aircraft. A concept of automatic flight control which is now evolving aims at the automation of nearly all traditional piloting functions, leaving the flight crew to exercise chiefly managerial and supervisory control over the system.

Many diverse and complex research problems arise in the design of such a flight control system. The problem studied in this paper deals with the automatic guidance of the aircraft in the horizontal plane. The most often encountered problems in horizontal guidance, which in current terminal area operations are largely solved jointly by the pilot and the air traffic controller, can be classified into three types: a) flying from an initial point and heading to a specified final point and heading; b) flying from an initial point and heading to intercept, and then fly along a line of specified heading; and c) flying from an initial point and heading to a specified final point with arbitrary final heading.

The three problems previously defined have particular significance in terminal area guidance. Problems of type b occur when the aircraft is to capture an ILS beam or when

it is to acquire and then fly along a particular VOR radial. If in addition the aircraft is to capture the beam or acquire the radial at a specified point, the guidance problem is of type a. In the ILS beam capture maneuver such a point might be the outer marker.

Many more complicated horizontal guidance problems can often be interpreted as a sequence of these three types of problems. For example, a holding pattern can be generated by flying in a specified sequence through a set of way points, where the guidance problem from one-way point to another is interpreted as a problem of type a or c, the choice depending on whether or not the heading of the aircraft when it arrives at the way points is specified or free. Similarly, guidance along entire flight profiles from takeoff to landing can be divided into a sequence of problems a, b, and c. The solution of these three guidance problems therefore assumes some importance in the development of an automatic guidance system and hence, is the subject of this paper.

In addition to horizontal guidance, vertical guidance and airspeed management must also be performed by the flight control system. However, except in special flight situations, horizontal guidance can be performed independent of vertical guidance and airspeed management, and this assumption will be used throughout this paper.

The three guidance problems defined here have the drawback of admitting an infinite number of flight trajectories for their solution. For example, in flying an aircraft from an initial position and heading to some specified final position and heading, a pilot may use a few steep turns and a number of straight-flight sections, or he may use several gently curved